



HAL
open science

Heterologous expression of a plant uracil transporter in yeast: improvement of plasma membrane targeting in mutants of the Rsp5p ubiquitin protein ligase.

Marine Froissard, Naïma Belgareh-Touzé, Nicole Buisson, Marcello Desimone, Wolf B. Frommer, Rosine Haguenauer-Tsapis

► To cite this version:

Marine Froissard, Naïma Belgareh-Touzé, Nicole Buisson, Marcello Desimone, Wolf B. Frommer, et al.. Heterologous expression of a plant uracil transporter in yeast: improvement of plasma membrane targeting in mutants of the Rsp5p ubiquitin protein ligase.. *Biotechnology Journal*, 2006, 1(3), pp.308-320. hal-00020527

HAL Id: hal-00020527

<https://hal.science/hal-00020527>

Submitted on 13 Mar 2006

HAL is a multi-disciplinary open access archive for the deposit and dissemination of scientific research documents, whether they are published or not. The documents may come from teaching and research institutions in France or abroad, or from public or private research centers.

L'archive ouverte pluridisciplinaire **HAL**, est destinée au dépôt et à la diffusion de documents scientifiques de niveau recherche, publiés ou non, émanant des établissements d'enseignement et de recherche français ou étrangers, des laboratoires publics ou privés.

1
2
3 1 **Heterologous expression of a plant uracil transporter in yeast: improvement of**
4
5
6 2 **plasma membrane targeting in mutants of the Rsp5p ubiquitin protein ligase**

7
8 3 Froissard M[&], Belgareh-Touzé N[&], Buisson N[&], Desimone M[°], Frommer WB^{\$} and
9
10
11 4 Haguenaer-Tsapis R^{&*}.

12
13
14
15 5 [&]Institut Jacques Monod-CNRS, Université Paris VI and Paris VII 2 place Jussieu
16
17 6 75251 Paris Cedex 05 France

18
19 7 [°] Plant Physiology, ZMBP, Auf der Morgenstelle 1, D-72076 Tübingen, Germany.

20
21
22 8 ^{\$}Carnegie Institution of Washington, Plant Biology, Stanford, California 94305-4101,
23
24 9 USA.

25
26
27 10 **Running title:** Functional expression of a plant transporter in yeast

28
29 11 *Corresponding author:

30
31 12 Tel: 33 1 44 27 63 86

32
33 13 Fax: 33 1 44 27 59 94

34
35 14 E mail: haguenaer@ijm.jussieu.fr

36
37
38 15

39
40
41 16 Keywords: transporters, yeast, heterologous expression, Rsp5p, ubiquitin protein
42
43 17 ligase

44
45
46 18

1
2
3
4
5
6
7
8
9
10
11
12
13
14
15
16
17
18
19
20
21
22
23
24
25
26
27
28
29
30
31
32
33
34
35
36
37
38
39
40
41
42
43
44
45
46
47
48
49
50
51
52
53
54
55
56
57
58
59
60

18 **Abstract:**

19 Plasma membrane proteins involved in transport processes play a crucial role in cell
20 physiology. On account of these properties, these molecules are ideal targets for
21 development of new therapeutic and agronomic agents. However, these proteins are
22 of low abundance, which limits their study. Although yeast seems ideal for expressing
23 heterologous transporters, plasma membrane proteins are often retained in
24 intracellular compartments. We tried to find yeast mutants potentially able to improve
25 functional expression of a whole set of heterologous transporters. We focused on
26 *Arabidopsis thaliana* ureide transporter 1 (AtUPS1), previously cloned by functional
27 complementation in yeast. Tagged versions of AtUPS1 remain mostly trapped in the
28 endoplasmic reticulum and were able to reach slowly the plasma membrane. In
29 contrast, untagged AtUPS1 is rapidly delivered to plasma membrane, where it
30 remains in stable form. Tagged and untagged versions of AtUPS1 were expressed in
31 cells deficient in the ubiquitin ligase Rsp5p, involved in various stages of the
32 intracellular trafficking of membrane-bound proteins. *rsp5* mutants displayed further
33 plasma membrane stabilization of untagged AtUPS1, and improved steady state
34 amounts of tagged versions of AtUPS1. *rsp5* cells are thus powerful tools to solve the
35 many problems inherent in heterologous expression of membrane proteins in yeast,
36 including ER retention.

1
2
3 38 **Introduction:**
4
5
6 39
7

8 40 Systematic sequencing of the genomes of complex organisms (e.g., the plant
9
10 41 *Arabidopsis thaliana*, certain parasites, and man) has revealed a great number of
11
12 42 genes that are likely to code for membrane transporters [1]. Many of these proteins
13
14 43 are assigned to this functional category on the sole basis of sequence similarity to
15
16 44 known transport proteins. Their biochemical properties are thus unknown and
17
18 45 information regarding substrate specificity is often lacking. To possess such
19
20 46 knowledge would be important both scientifically and industrially, because transport
21
22 47 proteins (channels, pumps, and carriers) play a crucial role in cell physiology. This is
23
24 48 illustrated by the numerous genetic diseases that are caused by defective transport
25
26 49 systems. Furthermore, cell surface membrane transporters may be ideal targets for
27
28 50 the development of new therapeutic or agronomic agents. Biological systems are
29
30 51 thus required for the functional expression of each transport protein and for the study
31
32 52 of its biochemical properties by means of quick, simple tests. The yeast
33
34 53 *Saccharomyces cerevisiae* expression system best meets these requirements. It is
35
36 54 easy to use and inexpensive, its "transportome" has been extensively analyzed *in*
37
38 55 *silico* [2,3] and the function of over 150 yeast transport proteins has been identified
39
40 56 [4]. Moreover, the construction of a complete collection of strains deleted for each of
41
42 57 the 6200 yeast genes [5] led to an impressive number of *S. cerevisiae* mutants
43
44 58 deficient in the transport of compounds as diverse as inorganic ions, metabolites, and
45
46 59 drugs. The phenotypes of these mutants are easily identified after growth on solid
47
48 60 media and have been used extensively in complementation tests, notably to clone
49
50 61 and characterize heterologous transporters.
51
52
53
54
55
56
57
58
59
60

1
2
3
4 62 Hundreds of plant transporters have been successfully cloned by
5
6 63 complementation in yeast [6-9]. The yeast system has also been used in biochemical
7
8 64 approaches, for example, to analyze the functional properties of plant H⁺-ATPases
9
10 65 [10]. Nevertheless, although yeast seems ideal for expressing plasma membrane
11
12 66 proteins including transporters and receptors, investigators often found some of
13
14 67 these proteins to be inactive in yeast, sometimes because the protein did not fold
15
16 68 properly and/or was not delivered to the plasma membrane but accumulated in a
17
18 69 secretory compartment (endoplasmic reticulum (ER), Golgi apparatus, secretory
19
20 70 vesicles), sometimes even leading to formation of karmellae [11]. On the other hand,
21
22 71 some heterologous proteins correctly delivered to the plasma membrane have been
23
24 72 described to undergo rapid endocytosis and turnover, resulting in low plasma
25
26 73 membrane levels [12].

27
28
29
30
31
32 74 A few attempts to improve functional expression in yeast of heterologous
33
34 75 plasma membrane transporters have been reported, but they often focused on only
35
36 76 one given transporter [13,14]. Attempts to identify yeast mutants that would
37
38 77 potentially improve the functional expression of a whole set of plasma membrane
39
40 78 proteins and more specifically transporters, are still lacking. Finding such mutants for
41
42 79 improvement of the functional expression of several plant and mammalian
43
44 80 transporters was the objective of an European network, EFFEXPORT ("Engineering
45
46 81 yeast for efficient expression of heterologous membrane transporters"). We report
47
48 82 here data we obtained within EFFEXPORT in the case of the *Arabidopsis Thaliana*
49
50 83 ureide transporter (AtUPS1), already known to be functionally expressed in *S.*
51
52 84 *cerevisiae* [15]. AtUPS1, was identified by functional complementation of a yeast *dal4*
53
54 85 *dal5* mutant [15] defective in uptake of allantoin. AtUPS1 belongs to a superfamily of
55
56 86 plant transporters with five members in Arabidopsis. Analysis of hydrophobicity

1
2
3 87 predicts 10 putative transmembrane domains, with N- and C-termini predicted to
4
5 88 protrude into the extracellular space. UPS proteins display a conserved central
6
7
8 89 domain between predicted transmembrane helices 5 and 6, which contains a
9
10 90 consensus sequence for a P loop, also designated as a « Walker A » motif for ATP
11
12 91 binding [15]. Expression in yeast and *Xenopus* oocytes allowed to demonstrate that
13
14 92 *AtUPS1* mediates uptake of allantoin and related metabolites including uracil [15,16].
15
16 93 The fate of *AtUPS1* can thus be compared to that of the endogenous uracil
17
18 94 permease (*Fur4p*), a well-known yeast transporter, the trafficking of which has been
19
20 95 studied extensively (reviewed in [17]). *Fur4p*, which belongs to a family of five
21
22 96 homologous proteins in *S. cerevisiae* [2], also consists of ten transmembrane spans,
23
24 97 with cytoplasmic oriented N- and C- termini [18]. Like most yeast plasma membrane
25
26 98 proteins, it displays plasma membrane ubiquitylation, catalyzed by the *Rsp5p*
27
28 99 ubiquitin protein ligase, a modification triggering its internalization and subsequent
29
30 100 vacuolar degradation [19]. The same ubiquitin ligase, the sole member of the family
31
32 101 of *Nedd4* ubiquitin ligases in yeast [20], was also demonstrated to be required for
33
34 102 direct Golgi-to-vacuole trafficking of a number of plasma membrane transporters,
35
36 103 including *Fur4p* [17,21], *i.e.* proteins routed to a direct degradation pathway
37
38 104 bypassing the plasma membrane under certain nutrient/substrate conditions. *Rsp5p*
39
40 105 was also described to be required for Golgi-to-vacuole traffic of misfolded plasma
41
42 106 membrane proteins misrouted to the vacuole [22]. In latter two cases, these proteins
43
44 107 were retargeted to plasma membrane in *rsp5* mutants. *rsp5* mutants thus display
45
46 108 increased steady state amounts of many plasma membrane transporters (reviewed
47
48 109 in [17]), and were good candidates for potential improvement of functional expression
49
50 110 of heterologous transporters. However, in addition to its role in trafficking of
51
52 111 membrane proteins [17], *Rsp5p* has many other functions, including essential
53
54
55
56
57
58
59
60

1
2
3 112 functions [23,24]. Hence, only defined *rsp5* mutants may be used for optimization of
4
5 113 functional expression of heterologous proteins. Two viable *rsp5* mutants that were
6
7
8 114 described to be affected for several of the trafficking functions of Rsp5p appeared
9
10 115 interesting: *npi1* mutant, with altered *RSP5* promoter, leading to a 10-fold reduction in
11
12 116 the steady state amount of this protein [25], and *rsp5ΔC2*, lacking Rsp5p C2 domain
13
14 117 involved in localization of the enzyme at plasma membrane and endosomes [26].
15
16
17

18
19 118 We report here an analysis of the fate of AtUPS1, as compared to that of
20
21 119 Fur4p, in wild type and *rsp5* mutant cells, and show that *npi1* and *rsp5ΔC2* cells
22
23 120 improved functional expression of the plant transporter.
24
25
26

27 121

28 29 122 **Results**

30 123

31 124 **AtUPS1 mediates high affinity uracil transport in yeast**

32
33
34
35
36 125 As outlined above, when expressed in yeast, AtUPS1 transports [¹⁴C] labelled
37
38 126 allantoin with high affinity and potentially other heterocyclic compounds as suggested
39
40 127 by competition studies [15]. Moreover, AtUPS1 mediates uracil uptake when
41
42 128 expressed in *Xenopus* oocytes [16]. In order to monitor the intracellular fate of
43
44 129 AtUPS1 in yeast, *UPS1* was cloned in a multicopy plasmid under the control of the
45
46 130 galactose-inducible GAL promoter. We defined the characteristics of uracil uptake
47
48 131 mediated by GAL-*UPS1*, as compared to uracil uptake mediated by the endogenous
49
50 132 Fur4p cloned under the control of the same promoter. *fur4Δ* cells grown on galactose
51
52 133 expressing either GAL-*UPS1* or GAL-*FUR4* displayed high sensitivity to 5-fluorouracil
53
54 134 (5FU), a toxic analog of uracil: cells expressing the transporters were unable to grow
55
56 135 on plates containing 1μM 5FU, whereas cells transformed with a control plasmid
57
58
59
60

1
2
3 136 grew normally (Fig 1A). To determine the uracil transport properties of AtUPS1
4
5
6 137 quantitatively, radiotracer uptake studies were performed using [^{14}C] uracil. [^{14}C]
7
8 138 uracil uptake mediated by GAL-*UPS1* expressed in *fur4* Δ cells growing exponentially
9
10
11 139 and fully induced on galactose was linear for at least 3 min, concentration-
12
13 140 dependent, and displayed saturation kinetics with an apparent K_m of 6 μM , close to
14
15
16 141 that observed in parallel for cells expressing GAL-*FUR4* (7.5 μM). *fur4* Δ cells
17
18 142 expressing GAL-*UPS1* grown overnight in galactose containing media displayed an
19
20
21 143 activity 50% of cells expressing GAL-*FUR4*, *i.e.*, more than 30-fold that of
22
23 144 chromosomal encoded *FUR4* (Fig. 1B), thus providing a sensitive assay to follow
24
25 145 AtUPS1 intracellular fate.
26
27
28 146

30 147 **Insight into AtUPS1 intracellular trafficking in yeast**

32 148 Inducibility of AtUPS1 synthesis after galactose induction provides a useful
33
34
35 149 tool for monitoring plasma membrane delivery, as previously demonstrated for the
36
37 150 yeast Fur4p [27]. We measured uracil uptake activity after galactose induction of
38
39
40 151 GAL-*UPS1* and GAL-*FUR4* in *fur4* Δ cells in parallel (Fig. 2A). In both cases, activity,
41
42 152 as a measure of plasma membrane targeting, was detectable after 30 min induction.
43
44
45 153 The increase in uracil uptake activity was linear for one hour with a similar slope for
46
47 154 cells expressing the yeast and the plant transporters. Hence the heterologous
48
49 155 AtUPS1 appears to be recognized efficiently by the yeast secretory machinery. We
50
51 156 then compared the fate of AtUPS1 and Fur4p along the endocytic pathway using an
52
53
54 157 experimental condition known to trigger rapid Fur4p internalization and subsequent
55
56 158 vacuolar degradation, *i. e.* the inhibition of protein synthesis by addition of
57
58 159 cycloheximide [28] (Fig. 2B). Cycloheximide was added to exponentially growing
59
60 160 *fur4* Δ cells induced overnight in galactose for expression of either AtUPS1 or Fur4p.

1
2
3 161 Uracil uptake activity of cells expressing Fur4p decreased rapidly ($t_{1/2} = 45$ min),
4
5
6 162 whereas uracil uptake activity of cells expressing AtUPS1 did not display a decrease
7
8 163 for four hours. Hence, once delivered to the plasma membrane, the plant AtUPS1
9
10 164 was remarkably stable, and did not undergo obvious endocytosis after inhibition of
11
12 165 protein synthesis.
13
14
15 166

17 167 **C-terminally tagged versions of AtUPS1 are retained in the ER**

18
19
20 168 The monitoring of uracil uptake activity can afford insight into the intracellular
21
22 169 fate of AtUPS1, since it provides information about the plasma membrane located
23
24 170 transporter. This information, however, remains limited, and does not indicate the
25
26 171 fraction of plasma membrane-delivered protein versus potential intracellular pools. In
27
28 172 the absence of available antibodies, we decided to monitor the fate of tagged
29
30 173 versions of AtUPS1. C-terminally tagged versions of AtUPS1 were constructed, first
31
32 174 with a GFP-tag, a powerful tool for monitoring the intracellular fate in yeast of plasma
33
34 175 membrane proteins of heterologous [14] or endogenous origin, including that of
35
36 176 Fur4p [29-31]. *fur4Δ* cells transformed with a multicopy plasmid carrying *GAL-UPS1-*
37
38 177 *GFP* displayed high 5FU sensitivity after growth on galactose (Fig. 3A). Strikingly,
39
40 178 *fur4Δ* cells transformed with multicopy plasmid carrying *GAL-UPS1* tagged with the
41
42 179 smaller HA epitope displayed intermediate 5FU sensitivity after growth on galactose,
43
44 180 indicating that a smaller tag did not improve AtUPS1 functionality. According to these
45
46 181 plate assays, C-terminally tagged AtUPS1 thus appeared functional, notably GFP-
47
48 182 tagged AtUPS1. However, *fur4Δ* cells transformed by the multicopy plasmid carrying
49
50 183 *GAL-UPS1-GFP* and fully induced displayed only a very low level of uracil uptake
51
52 184 activity (0.04 nMol/min/A₆₀₀), an activity 50 fold lower than that observed in the case
53
54 185 of induced cells transformed by a plasmid carrying untagged AtUPS1 (not shown).
55
56
57
58
59
60

1
2
3 186 The use of a smaller tag (HA) or another promoter (CYC1) did not improve uracil
4
5 187 uptake activity.
6
7

8 188 The GFP -or HA- tags may inhibit transport activity or impair plasma
9
10 189 membrane delivery of tagged transporter due to folding problems. We checked GFP
11
12 190 fluorescence in time course experiments using the multicopy plasmid carrying the
13
14 191 *GAL-UPS1-GFP* (Fig. 3B), or the multicopy plasmid *GAL-Fur4-GFP* as a control.
15
16 192 Galactose induction of *Fur4-GFP* led, after 30 min, to observation of small internal
17
18 193 compartments, likely Golgi/secretory vesicles. 30 min later, plasma membrane
19
20 194 staining was clearly evidenced, often in a polarized fashion, with intense staining of
21
22 195 small buds (Fig. 3B). The distribution of *AtUPS1-GFP* was strikingly different. After
23
24 196 30 min of galactose induction of *AtUPS1-GFP* expression, a perinuclear staining was
25
26 197 clearly observable. 30 min later, or after overnight induction, the perinuclear staining
27
28 198 was still present and a discontinuous staining at/or underneath the plasma
29
30 199 membrane has appeared. This pattern is typical of the yeast ER. Intense staining of
31
32 200 lines or spots, as if intracellular membranes had formed aggregates were also
33
34 201 visualized (Fig. 3B). Indeed, electron microscopy of the ultrastructural morphology of
35
36 202 cells fully induced for expression of *AtUPS1-GFP* revealed proliferation, hanks of ER
37
38 203 membranes (Fig. 3D), as often described in the case of cells overexpressing ER-
39
40 204 retained proteins [11]. This altered morphology did not resulted from the
41
42 205 overexpression of a membrane protein as such: overnight overexpression of
43
44 206 endogenous *FUR4* from the same multicopy, GAL-inducible plasmid, did not lead to
45
46 207 altered morphology (not shown).
47
48
49
50
51
52
53

54
55 208 ER-retention of GFP-tagged *AtUPS1* apparently did not result from the mere
56
57 209 overexpression of this protein. Perinuclear/ER staining was also evidenced upon
58
59 210 expression of *AtUPS1-GFP* from a centromeric plasmid under the control of the mild
60

1
2
3 211 strength *CYC1* promoter, leading to a steady state protein level about 4-fold lower
4
5 212 than that observed after two hours galactose induction of GAL-*UPS1-GFP* (Fig. 3B
6
7 213 and C). Furthermore, when analyzed by sucrose gradient fractionation, AtUPS1-GFP
8
9 214 expressed from the CEN *CYC1*-plasmid or from the 2 μ GAL-inducible plasmid
10
11 215 displayed exactly the same pattern with major pool in internal fractions (data not
12
13 216 shown).

14
15
16
17 217 Hence, the GFP tag at the C-terminus of AtUPS1 obviously triggers ER
18
19 218 retention of the transporter. The low uracil uptake activity of cells expressing this
20
21 219 transporter can only be observed after long expression periods (3-4 hours, cf Fig.
22
23 220 6B), and likely corresponds to the low fraction of protein finally reaching the plasma
24
25 221 membrane. With such folding problems, overexpression is a way to increase steady
26
27 222 state plasma membrane expression: both 5FU sensitivity and uracil uptake activity
28
29 223 were improved in the case of AtUPS1-GFP expression from a multicopy plasmid and
30
31 224 strong GAL promoter compared to expression from a centromeric plasmid under the
32
33 225 control of a lower strength promoter.
34
35
36
37
38
39
40

41 227 **Intracellular fate of AtUPS1 carrying an internal myc tag in yeast: slow ER exit** 42 43 228 **but final plasma membrane delivery**

44
45
46 229 We checked whether insertion of a small myc-tag inside the central loop
47
48 230 containing the Walker A motif would be a better way to study AtUPS1 intracellular
49
50 231 trafficking. Cells expressing internally myc tagged AtUPS1 from a multicopy
51
52 232 galactose inducible plasmid displayed high sensitivity to 5FU (Fig. 4A). Cells
53
54 233 transformed with the multicopy GAL-*UPS1^{myc}* plasmid grown overnight in galactose
55
56 234 displayed a relatively high level of uracil uptake activity: 1 nMol/min/A₆₀₀, *i. e.* 70%
57
58 235 that observed in the case of untagged AtUPS1 (Fig. 4B), suggesting that the myc tag
59
60

1
2
3 236 at this position had only a small impact on AtUPS1 function. However, this tag had a
4
5 237 clear influence on AtUPS1 intracellular trafficking. Induction experiments showed that
6
7 238 uracil uptake activity appeared slowly: 4-6 hours were necessary before we were
8
9 239 able to measure any detectable uptake activity (Fig. 4C). Aliquots withdrawn at
10
11 240 several time points after galactose induction were analyzed by protein gel blots using
12
13 241 a specific anti-myc antibody. AtUPS1^{myc} appeared on gels as a band of apparent
14
15 242 molecular mass of about 36 kDa, *i. e.* slightly below the expected molecular mass
16
17 243 deduced from predicted protein sequence (44 kDa) (Fig. 4E), as often observed for
18
19 244 very hydrophobic proteins. A comparable pattern was observed after overnight
20
21 245 galactose induction of AtUPS1^{myc} expressed from either a centromeric or a multicopy
22
23 246 plasmid (data not shown).

24
25
26
27
28
29
30 247 In order to check the intracellular location of AtUPS1^{myc} derived species, cells
31
32 248 transformed with GAL-UPS1^{myc} were induced by addition of galactose, aliquots
33
34 249 withdrawn periodically were fixed and analyzed by immunofluorescence using a
35
36 250 monoclonal anti-myc antibody. One hour induction was sufficient to observe a
37
38 251 specific signal, mostly perinuclear, supported by simultaneous DAPI staining (Fig.
39
40 252 5A). To obtain better resolution of the cell surface staining (potentially corresponding
41
42 253 to either ER or plasma membrane), cells were examined by confocal microscopy.
43
44 254 The lower background in optical slices made it possible to show that all cells
45
46 255 displayed perinuclear staining, together with discontinuous regions of cell surface
47
48 256 staining (Fig. 5B). Because cell surface was not homogeneously stained, we can
49
50 257 conclude that the main signal corresponds to ER staining and that a plasma
51
52 258 membrane localisation cannot be detected by this approach. The low rate of uracil
53
54 259 uptake activity thus likely resulted from low ER exit rates (Fig. 4C) The finding that
55
56 260 the activity of fully induced cells is in a similar range as that of cells expressing

1
2
3 261 untagged AtUPS1, which was rapidly targeted to plasma membrane, may suggest
4
5 262 that after slow rates of ER exit, AtUPS1^{myc} finally reached the plasma membrane.
6
7 263 Further indication that AtUPS1^{myc} stored in internal compartments could finally reach
8
9 264 plasma membrane was provided by the observation of some increase in uracil
10
11 265 uptake activity after stopping transporter synthesis by the addition of CHX (Fig. 4D).
12
13 266 Once targeted at the plasma membrane, AtUPS1^{myc} was rather stable, as judged
14
15 267 from the extreme stability of uracil uptake activity for over 3 hours after this transient
16
17 268 uracil uptake activity increase following CHX addition. However, some low rate
18
19 269 endocytosis likely occurred as compared to the incredibly stable untagged AtUPS1
20
21 270 (Fig. 4D).
22
23
24
25
26
27
28
29
30
31

32 273 **Mutations in the Rsp5 ubiquitin protein ligase improve functional expression of** 33 34 274 **tagged and untagged AtUPS1 in yeast**

35
36 275 Despite the difficulties encountered in tagging AtUPS1 at different positions,
37
38 276 the high sensitivity of the two functional tests, 5FU sensitivity and uracil uptake
39
40 277 measurements, provided suitable tools to check whether yeast mutants could
41
42 278 improve the steady state levels of functional tagged or untagged AtUPS1 versions.
43
44 279 We used two viable *rsp5* mutants, *npi1* and *rsp5ΔC2*, that display delayed
45
46 280 endocytosis of several cargoes, including Fur4p. Accordingly, they displayed
47
48 281 increased 5FU sensitivity as a result of the plasma membrane stabilization of
49
50 282 endogenous chromosomal or plasmid encoded Fur4p (not shown). We checked the
51
52 283 fate of tagged and untagged versions of AtUPS1 in *npi1* and *rsp5ΔC2* mutant cells.
53
54
55
56
57

58 284 For this purpose, *FUR4* was deleted in wild type, *npi1* and *rsp5ΔC2* cells, and
59
60 285 the resulting strains were transformed with multicopy plasmids carrying either *UPS1*

1
2
3 286 under the control of the constitutive PGK promoter (plasmid pFL61-*UPS1*), or
4
5 287 galactose inducible *UPS1*, *UPS1-GFP* and *UPS1^{myc}*. Transformed cells grown in
6
7
8 288 glucose, or galactose containing media in the case of plasmids with a GAL promoter
9
10 289 displayed identical growth in the absence of 5FU (Fig. 6A), indicating that neither the
11
12 290 mutations, nor the expression of the plant transporters impaired growth. 5FU
13
14 291 sensitivity of transformants was strikingly enhanced in both *rsp5ΔC2* and *npi1* cells
15
16 292 expressing the tagged and untagged plant transporter when compared to wild type
17
18 293 cells, with slightly stronger effect promoted in all cases by the *npi1* mutation
19
20 294 (compare the size of isolated colonies) (Fig. 6A). This suggests higher amounts of
21
22 295 plasma membrane tagged or untagged transporters in the mutants. In the case of the
23
24 296 untagged transporters, the enhancement in 5FU sensitivity was evidenced after
25
26 297 synthesis from PGK or *GAL10* promoter at different 5FU concentrations (Fig. 6A),
27
28 298 indicating that *rsp5* mutations interfered with trafficking, rather than with galactose-
29
30 299 driven expression. For untagged AtUPS1 which is rapidly delivered to the plasma
31
32 300 membrane and very stable in wild type cells, the increase in functional transporter
33
34 301 activity observed in *rsp5* α mutants may result from inhibition of some direct Golgi to
35
36 302 vacuole targeting, or from protection against a possible low basal endocytosis, for
37
38 303 instance when cells reached stationary phase, a likely situation for cells grown
39
40 304 several days on plates.
41
42
43
44
45
46
47

48 305 In the case of the myc-tagged version of AtUPS1, we monitored the fate of the
49
50 306 transporter after galactose induction by western blots (Fig 6C), and uracil uptake
51
52 307 measurements (Fig. 6B). In agreement with fluorescent data, AtUPS1^{myc} protein was
53
54 308 already detectable in wild type cells at early time points after induction (30-60 min)
55
56 309 but uracil uptake was readily measurable only at far later time points (4 hours). In
57
58 310 *npi1* cells, AtUPS1^{myc} was detectable in higher amounts at all time points and uracil
59
60

1
2
3 311 uptake activity appeared at least one hour earlier compared to wild type cells (Fig.
4
5 312 6B). *rsp5ΔC2* mutation also resulted in more rapid appearance of uracil uptake
6
7 313 activity. Strikingly, even if the activity was lower for cells expressing AtUPS1-GFP
8
9 314 compared to AtUPS1^{myc}, the rate of appearance of uptake was very similar. For both
10
11 315 types of tagged transporters uracil uptake activity was thus 2-3 fold higher in mutant
12
13 316 cells than in wild type cells after 4 hour induction. Since the major pool of both
14
15 317 AtUPS1-GFP and AtUPS1^{myc} seemed to be in the ER, both *npi1* and *rsp5ΔC2*
16
17 318 mutations apparently lead to accelerated ER exit.
18
19
20
21
22
23
24

319

320 Discussion:

321 The use of a regulable promoter and the high sensitivity of uracil uptake
322 measurements enabled us to obtain crucial information about the fate of untagged
323 AtUPS1 uracil transporter in yeast. AtUPS1 is rapidly delivered to the plasma
324 membrane, with kinetics indistinguishable from those of endogenous yeast
325 transporter. Hence, the yeast secretory pathway efficiently handles the heterologous
326 plant transporter. It is possible that such property was the reason for the successful
327 cloning by functional expression of so many plant transporters when using yeast as a
328 host system [6,7]. Plasma membrane delivered AtUPS1 exhibited striking stability,
329 notably when compared to the endogenous yeast uracil permease especially
330 susceptible to stress-induced endocytosis [28]. This was true for both untagged
331 transporter and for internally tagged AtUPS1^{myc} (not shown). This differential stability
332 between yeast and plant uracil transporters may possibly reflect fundamental
333 differences in their endocytic processes. Endocytosis in yeast is dependent on prior
334 ubiquitylation of plasma membrane cargoes by the Rsp5p ubiquitin protein ligase
335 [17]. A subset of mammalian proteins undergo ubiquitin-dependent endocytosis,

1
2
3 336 sometimes involving ubiquitin-protein ligases of the Nedd4/Rsp5 family [32]. In
4
5
6 337 contrast, although plants display numerous ubiquitin protein ligases, they do not
7
8 338 seem to have Rsp5p orthologs [33]. The extreme stability of AtUPS1 in yeast could
9
10 339 result from the absence or low accessibility of ubiquitylation sites that Rsp5p can
11
12 340 recognize, at least under the experimental conditions we tested. One possible reason
13
14
15 341 could be the luminal orientation of both AtUPS1 N- and C-termini.
16

17 342 In addition to obtaining information on intracellular trafficking of the plant
18
19 343 AtUPS1 in yeast based on uptake measurements, we tried to gain new insights into
20
21 344 the biochemical properties of this transporter. Unfortunately, tagging the transporter,
22
23 345 either at the N-terminus (not shown) and C-terminus or inside its central loop, lead to
24
25 346 folding problems, often resulting in ER retention of most of the protein, preventing us
26
27 347 from using these tagged versions to obtain a judicious biochemical characterization
28
29 348 of this transporter. A marked difference, however, was observed between internal
30
31 349 tagging, and tagging at the N- and C-termini, which was far more deleterious.
32
33 350 Internally tagged transporter displayed delayed ER exit, but finally reached the
34
35 351 plasma membrane in a fully functional state, and fully induced cells expressing this
36
37 352 version of the transporter displayed activity closely resembling that of cells
38
39 353 expressing untagged transporter. In contrast, cells expressing C-terminally tagged
40
41 354 transporter displayed 40-fold less uracil uptake activity compared to cells expressing
42
43 355 untagged transporters, probably because of a very low percentage of the protein
44
45 356 exiting the ER. In latter case, some improvement could be achieved by increased
46
47 357 levels of expression (stronger promoter, multicopy versus centromeric plasmid). The
48
49 358 deleterious effect of C-terminal tags could result from the unusual structure of the
50
51 359 transporter. Hydrophobicity plot analysis of proteins of the UPS family suggested an
52
53 360 external orientation of both termini [15] a situation somewhat rare for transporters.
54
55
56
57
58
59
60

1
2
3 361 Most yeast transporters, for instance, display cytoplasmic oriented termini, as
4
5 362 predicted from hydrophobicity plot analysis or from experimental data [2]. Many of
6
7 363 these transporters were studied after tagging, most often at their C-terminus, a
8
9 364 modification that did not induce any major trafficking problems. The observation that
10
11 365 N- and C-terminal tags impaired AtUPS1 folding is compatible with an external
12
13 366 orientation, but experimental data are required to prove this. One obvious lesson
14
15 367 from these observations is that tagging at the positions and with the tags used in the
16
17 368 present study may probably influence the fate of UPS proteins in plant cells in a
18
19 369 similar way as in yeast cells. Indeed, previous studies attempting to study the
20
21 370 subcellular location of N- or C-terminal fusions of UPS proteins with GFP by transient
22
23 371 expression in Arabidopsis protoplasts showed that these fusion proteins did not
24
25 372 reach the plasma membrane (Schmidt, A., Baumann, N. and Desimone, M.,
26
27 373 unpublished data). This suggests that yeast may also represent a useful
28
29 374 experimental system to decipher where tags can be introduced in heterologous
30
31 375 transporters.
32
33
34
35
36
37
38

39 376 The distinctive behaviour of the various versions of AtUPS1, one correctly
40
41 377 targeted to the plasma membrane, and two retained in the ER to various extents,
42
43 378 provided the opportunity to check how to improve the steady state plasma membrane
44
45 379 amount of heterologous transporters with distinct intracellular fates. We checked
46
47 380 specifically the influence of mutations in Rsp5p. This ubiquitin protein ligase is
48
49 381 involved in various stages of intracellular trafficking of membrane-bound proteins,
50
51 382 including ER-associated degradation, plasma membrane internalization, Golgi to
52
53 383 vacuolar trafficking, and sorting to multivesicular bodies [17]. Limiting or preventing
54
55 384 latter three trafficking steps results in elevated steady state levels of yeast
56
57 385 transporters. Two specific viable mutants were used, *npi1*, with decreased amounts
58
59
60

1
2
3 386 of Rsp5p [25] and *rsp5ΔC2*, lacking the C2 domain of Rsp5p [34], dispensable for
4
5
6 387 viability, but critical for Rsp5p trafficking functions [26,34-38]. Strikingly, both mutants
7
8 388 improved steady state amounts of functional, plasma membrane targeted, tagged
9
10 389 and untagged versions of AtUPS1, as judged from increased 5FU sensitivity. In the
11
12 390 case of untagged transporter, increased 5FU sensitivity was observed after
13
14
15 391 expression of the transporter under the control of the constitutive PGK promoter, or
16
17 392 the inducible *GAL10* promoter, indicating that the mutations interfered as expected
18
19 393 with trafficking rather than with expression.
20
21

22 394 In the case of the untagged version of AtUPS1, it was difficult to further
23
24 395 explore the mechanism of this improvement. Plasma membrane AtUPS1 was so
25
26 396 stable in wild type cells submitted to CHX treatment that further stabilisation in *rsp5*
27
28 397 cells could not be detected in this type of experiment. The improvement in plasma
29
30 398 membrane steady state amounts of AtUPS1 in *npi1* and *rsp5ΔC2* cells might possibly
31
32 399 arise from a low basal endocytosis of AtUPS1, undetectable in CHX chase
33
34 400 experiments, but possibly occurring once cells reach stationary phase, as is the case
35
36 401 for cells grown on plates. Alternatively, the increase in plasma membrane AtUPS1 in
37
38 402 these *rsp5* mutants could result from a decreased direct Golgi to vacuole targeting of
39
40 403 a fraction of the transporter.
41
42
43
44
45

46 404 Mutations in *RSP5*, either *npi1* or *rsp5ΔC2*, had a similar impact on the
47
48 405 intracellular fate of tagged versions of AtUPS1 at both the C-terminus or in the
49
50 406 intracellular loop. These two variants of AtUPS1 were mainly located in the ER, with
51
52 407 possibly exit in only very limited amounts (AtUPS1-GFP), or more important final
53
54 408 amounts (AtUPS1^{myc}) thus leading to uracil uptake activity similar to that displayed by
55
56 409 cells expressing untagged transporters. In both cases, the rate of plasma membrane
57
58 410 delivery of uracil uptake activity was greatly delayed, with activity measurable after 3-
59
60

1
2
3 411 4 hours induction instead of 30 min for AtUPS1 –i. e. long after detection of the
4
5 412 protein on Western blots- and the two *rsp5* mutations reduced this delay. At first
6
7 413 glance, this effect can be attributed to an effect of Rsp5p on ER exit. Among its many
8
9 414 functions, Rsp5p was described to be involved in ubiquitylation followed by
10
11 415 proteasome degradation of several misfolded soluble and membrane-bound proteins
12
13 416 retained in the ER, notably under conditions of saturation of other ER-associated
14
15 417 degradative (ERAD) pathways [39]. Tagged forms of AtUPS1 might be partly
16
17 418 susceptible to such an Rsp5p-dependent ER-associated degradation, and inhibition
18
19 419 of this degradation in *npi1* and *rsp5ΔC2* mutants would result in more rapid ER exit of
20
21 420 transporters escaping this degradation to some extent. It is also possible that a small
22
23 421 number of misfolded tagged transporters undergo ER to Golgi trafficking, followed by
24
25 422 Golgi to vacuole sorting. Rsp5p was also shown to be involved in Golgi to vacuole
26
27 423 trafficking of some misfolded mutant plasma membrane proteins [22] or of yeast
28
29 424 transporters displaying direct vacuolar targeting under specific nutrient conditions
30
31 425 [17]. In both cases in *rsp5* mutants, these proteins are directed to plasma membrane
32
33 426 [22,40]. A small fraction of tagged AtUPS1 could undergo such direct vacuolar
34
35 427 trafficking, a process inhibited in *rsp5* mutants. In support of a partial direct Golgi to
36
37 428 vacuole trafficking of AtUPS1^{myc}, we observed that *pep4* mutant cells, deficient for
38
39 429 vacuolar protease activities, displayed higher amounts of the 36 kDa AtUPS1^{myc}
40
41 430 species than wild type cells even after short induction times, as did *vps23Δ* mutants,
42
43 431 impaired in Golgi to vacuole trafficking (data not shown). The increase in plasma
44
45 432 membrane amounts of functional forms of tagged AtUPS1 in *rsp5* mutants, attested
46
47 433 in exponentially growing cells by increased uracil uptake activity, and on plates by
48
49 434 increased 5FU sensitivity might also result from an inhibition of Rsp5p-dependent
50
51
52
53
54
55
56
57
58
59
60

1
2
3 435 processes at three levels: ERAD, Golgi-to-vacuole trafficking and plasma membrane
4
5 436 internalization.

7 437 Rsp5p plays a key role in trafficking of yeast plasma membrane proteins. The
8
9
10 438 present study shows that several viable *rsp5* mutants display increased plasma
11
12 439 membrane amounts of a plant transporter, rapidly targeted to the plasma membrane.
13
14 440 Strikingly, within the same european network (EFFEXPORT), other laboratories
15
16 441 observed, in viable *rsp5* mutants, improved functional expression of several
17
18 442 heterologous transporters, including several NH_4^+ transporters (Rh family) of animal
19
20 443 origin (Marini A and André B, personal communication), and increased plasma
21
22 444 membrane amounts versus internal fractions of mammalian Na^+/H^+ antiporters
23
24 445 (Flegegova, H, Haguenaer-Tsapis, R and Sychrova, H. Biochem. Biophys. Acta, in
25
26 446 press). In addition, these mutants optimize plasma membrane delivery of tagged
27
28 447 versions of the plant AtUPS1, stacked in the ER as a result of folding problems. ER
29
30 448 retention is one of the major problems encountered in the case of expression of
31
32 449 heterologous plasma membrane proteins in yeast. The increase in steady state
33
34 450 plasma membrane amounts of heterologous plant and mammalian transporters,
35
36 451 upon expression in viable *rsp5* mutants, show that these cells could be powerful tools
37
38 452 to solve the many problems inherent in heterologous expression of membrane
39
40 453 proteins, including ER retention.
41
42
43
44
45
46
47
48
49

50 454

51 52 455 **Materials and methods**

53 456

54 457 *Yeast strains and growth conditions*

55
56
57 458 Yeast strains were transformed as described by Gietz et al [41]. Cells were grown at
58
59 459 30°C in minimal medium (YNB) containing 0.67% yeast nitrogen base without amino
60

1
2
3 460 acids (BD bioscience, NJ, USA), and supplemented with appropriate nutrients. The
4
5 461 carbon source was 2% glucose, or 2% galactose plus 0.05% glucose as indicated in
6
7 462 the figure legends. Galactose induction was performed on cells grown overnight in
8
9 463 2% raffinose plus 0.05% glucose up to an $A_{600nm}=0.5$. Galactose (2%) was then
10
11 464 added to the medium.
12

13
14 465 The disruption of *FUR4* gene was achieved by ORF replacement with long flanking
15
16 466 homology regions to the KanMX4 cassette corresponding to the strategy described
17
18 467 by Wach [42].
19

20
21
22 468

23 24 469 *Growth tests in the presence of 5-fluorouracil*

25
26 470 Cells, prototroph for uracil, were cultured overnight in minimal medium containing
27
28 471 glucose and spotted on plates containing minimal medium with galactose to induce
29
30 472 expression of *FUR4* or *UPS1* variants and supplemented with various concentrations
31
32 473 of 5FU (Sigma-Aldrich, Lyon, France). The first drop contained $3 \cdot 10^4$ cells and each
33
34 474 subsequent drop was diluted six-fold compared to the prior drop.
35
36 475

37
38
39 476

40 476 *Construction of plasmids*

41
42 477 DNA manipulations, including restriction analysis and ligations, were performed
43
44 478 essentially as described by Maniatis *et al.* [43].
45

46
47 479 The control plasmid p195gF-GFP (pRT208) expressing *FUR4*-GFP under the control
48
49 480 of the *GAL10* promoter was constructed by cloning a *Pst*I/*Bam*H1 fragment (*FUR4*-
50
51 481 GFP) from pFL38gF-GFP [30] into p195gF [28] at the *Pst*I/*Bam*HI site.
52

53
54 482 The pGAL-*UPS1* (pRT205) plasmid was constructed by insertion of a *Bam*HI/*Eco*RI
55
56 483 fragment encoding *UPS1* (with pFL61-*UPS1* as a template [15]) in the *Bam*HI/*Eco*RI
57
58 484 site of pYEF1 [44].
59
60

1
2
3 485 To construct the plasmid GAL-*UPS1-GFP* (pRT206) we first built the pNBT29
4
5 486 plasmid, which contains the yeast enhanced GFP under the control of the GAL10
6
7 487 promoter on a multicopy plasmid. For this purpose, a BamHI/NotI fragment encoding
8
9 488 GFP was obtained by PCR using the pUG35 plasmid as a template [45] and
10
11 489 introduced at the BamHI/NotI site of pYEF1 [44]. Then a BamHI/ClaI fragment
12
13 490 encoding AtUPS1 was amplified by PCR using pFL61-*AtUPS1* [15] as a template,
14
15 491 and introduced at the BamHI/ClaI site of pNBT29 in frame with the coding sequence
16
17 492 of GFP thereby creating a GFP C-terminally tagged version of AtUPS1. To construct
18
19 493 the *CYC1-UPS1-GFP* (pRT207) plasmid we cloned the BamHI/EcoRI fragment
20
21 494 containing *UPS1-GFP* at the BamHI/EcoRI site of the p416-CYC1 plasmid [46].
22
23 495 The pGAL-*UPS1-HA* (pRT204) plasmid was obtained by insertion in the ClaI site of
24
25 496 the pYEF2 [44], in frame with the coding sequence of the HA tag, of a fragment
26
27 497 encoding *UPS1* obtained by restriction of the plasmid GAL-*UPS1-GFP*.
28
29 498 To construct the plasmid pGAL-*UPS1^{myc}* (pRT203) two fragments of *UPS1* were
30
31 499 amplified separately by PCR using pFL61-*UPS1* as a template. One fragment
32
33 500 contained at start an EcoRI and an XbaI site, the 5'- portion of the *UPS1* coding
34
35 501 sequence (from ATG to the position 549) and a BamHI site at the end. The other
36
37 502 fragment contained a BamHI site at the start, the coding sequence for the c-myc
38
39 503 epitope, the 3'- portion of *UPS1* (from position 550 to the stop codon), and an EcoRI
40
41 504 and a XhoI site at the end. Both fragments were sequentially cloned in pDR199 [47]
42
43 505 using the EcoRI/BamHI sites for the first fragment and BamHI/and XhoI for the
44
45 506 second. After sequencing, the complete c-myc tagged *UPS1* sequence was obtained
46
47 507 by restriction and subcloned into the Xba I / Xho I sites of the CEN plasmid p416-
48
49 508 GAL [46]. Afterwards, the multicopy plasmid pGAL-*UPS1^{myc}* was obtained by
50
51
52
53
54
55
56
57
58
59
60

1
2
3 509 subcloning a SacI/XhoI fragment of the p416-GAL-*UPS1^{myc}* into the SacI/XhoI sites
4
5 510 of the p426-GAL plasmid [46].
6

7
8 511

9
10 512 *Measurement of uracil uptake.*

11
12 513 Uracil uptake was measured in exponentially growing cells as previously described.

13
14 514 Yeast culture (1 ml) was incubated with 5 μM [^{14}C] uracil (ICN biomedical Illkirch,

15
16 515 France) for 20 sec at 30°C, then quickly filtered through Whatman GF/C filters, which

17
18 516 were in turn washed twice with ice-cold water and counted for radioactivity. In the

19
20 517 case of low uracil uptake activity, this basic protocol was slightly modified, with the

21
22 518 use of two ml samples and incubation for 2 min at 30°C.
23
24
25
26

27 519

28
29 520 *Michaelis-Menten kinetics*

30
31 521 Uracil uptake activities measured at various substrate concentrations were fitted to a

32
33 522 hyperbola with SIGMA PLOT 5.0, V5 according to Michaelis-Menten kinetics.
34
35

36 523

37
38 524 *Yeast cell extracts, SDS-PAGE and Western immunoblotting*

39
40 525 Total protein extracts were prepared by the NaOH/Trichloroacetic acid (TCA) lysis

41
42 526 technique as described in [28]. Proteins were separated by SDS-PAGE on Tricine

43
44 527 gels and transferred onto nitrocellulose membranes. The membranes were probed

45
46 528 with monoclonal antibodies against GFP (Roche Diagnostics Meylan, France), or

47
48 529 myc (9E10 from Roche Diagnostics), or polyclonal antibody against Gas1p (a kind

49
50 530 gift from H. Riezman). Primary antibodies were detected using horseradish

51
52 531 peroxidase-conjugated anti-rabbit or anti-mouse IgG secondary antibody (Sigma-

53
54 532 Aldrich, Lyon, France) revealed by ECL chemiluminescence (Amersham).
55
56
57
58
59
60

533

1
2
3 534 *Immunofluorescence*
4

5 535 Immunofluorescence was performed as described in [48] except that cells were
6
7
8 536 permeabilized with 0.5% Triton X100. The primary antibody was the monoclonal anti-
9
10 537 Myc (9E10 from Roche Diagnostics, Meylan, France) and the secondary antibody
11
12 538 was an FITC-conjugated goat anti-mouse-IgG (Jackson ImmunoResearch
13
14 539 Laboratories, Inc., West Grove, PA). For DNA staining, 1 µg/ml Diamin-Phenylindol-
15
16 540 Dihydrochlorid (DAPI) was used. Samples were viewed under an Olympus
17
18 541 microscope BY61 using FITC and DAPI filter sets. Image acquisition was performed
19
20 542 using a Spot charge-coupled device camera SPOT4.05 .
21
22
23

24 543 For confocal analysis, cells were imaged using an inverted microscope (Leica, Inc.
25
26 544 Wetzlar, Germany) and scanning was performed with a True Confocal Scanner LEICA
27
28 545 TCS 4D.
29
30

31
32 546

33
34 547 *Electron microscopy*
35

36 548 Yeast cells were fixed by adding 200 µl of 50% aqueous glutaraldehyde to 10 ml of
37
38 549 growth medium for 10 min and then centrifuged at 5000 g for 10 min at 4°C. After
39
40 550 fixation with fresh fixatives for 2 h at 4°C, cells were washed in 0.1 M cacodylate
41
42 551 buffer (pH 7.4) and in water. Subsequently, cells were treated with 1% KMnO₄ for 2 h
43
44 552 on ice, washed in water and re-suspended in 2% aqueous uranyl acetate for 1 h at
45
46 553 4°C. Cells were dehydrated in a graded series of ethanol, infiltrated in a mixture of
47
48 554 ethanol and Spurr's resin and embedded in Spurr's low viscosity media. Thin
49
50 555 sections were cut, stained with lead citrate and examined in a Tecnai 12 electron
51
52
53 556 microscope (Eindhoven, Netherlands).
54
55
56

57
58 557
59
60

558

TABLE 1. List of strains

Strain	Background	Genotype	Source
MF04	Σ 1278b	<i>MATa ura3 trp1 FUR4::KanMX4</i>	This study
MF05	Σ 1278b	<i>MATa ura3 trp1 rsp5ΔC2 FUR4::kanMX4</i>	This study
MF06	Σ 1278b	<i>Mata ura3 trp1 npi1 FUR4::kanMX4</i>	This study
27061b	Σ 1278b	<i>Mata ura3 trp1</i>	[19]
27064b	Σ 1278b	<i>Mata ura3 trp1 npi1</i>	[19]
BY4741	BY	<i>Mata leu2Δ met15Δ ura3Δ his3Δ</i>	Euroscarf

559

560

561

TABLE 2. List of plasmids

Plasmid	Characteristics	Source
pPGK- <i>UPS1</i> (PFL61- <i>UPS1</i>)	2 μ , <i>URA3</i> prom. <i>PGK-UPS1</i>	[15]
pGAL (PYeF2)	2 μ , <i>URA3</i> , prom. <i>GAL10</i> , <i>Cter HA</i>	[44]
pGAL- <i>FUR4</i> (pFL38gF)	CEN, <i>URA3</i> , prom. <i>GAL10</i> , <i>FUR4</i>	[30]
p195gF	2 μ , <i>URA3</i> , prom. <i>GAL10</i> , <i>FUR4</i>	[28]
p195gF-GFP (pRT208)	2 μ , <i>URA3</i> , prom. <i>GAL10-FUR4-GFP</i>	This study
pGAL- <i>UPS1-HA</i> (pRT204)	2 μ , <i>URA3</i> , prom. <i>GAL10</i> , <i>UPS1-HA</i>	This study
pGAL- <i>UPS1</i> (pRT205)	2 μ , <i>URA3</i> , prom. <i>GAL10</i> , <i>UPS1</i>	This study
pGAL- <i>UPS1-GFP</i> (pRT206)	2 μ , <i>URA3</i> , prom. <i>GAL10</i> , <i>UPS1-GFP</i>	This study
pCYC1- <i>UPS1-GFP</i> (pRT207)	CEN, <i>URA3</i> , prom. <i>CYC1</i> , <i>UPS1-GFP</i>	This study
pGAL- <i>UPS1^{myc}</i> (pRT203)	2 μ , <i>URA3</i> , prom. <i>GAL10</i> , <i>UPS1-myc</i>	This study

562

1
2
3 563 **Figure 1: Comparison of uracil uptake activity of *Arabidopsis thaliana* UPS1**
4
5 564 **expressed in yeast and endogenous uracil permease Fur4p.**

6
7
8 565 A: 5-Fluorouracil (5FU) sensitivity. *fur4*Δ cells transformed with either pGAL (empty
9
10 566 vector), pGAL-*UPS1* or pGAL-*FUR4* were grown on galactose containing plates
11
12 567 supplemented or not with 1μM 5FU (toxic analog of uracil).

13
14
15 568 B: Uracil uptake activity of AtUPS1 compared to Fur4p. *fur4*Δ strains transformed
16
17 569 with pGAL (white), pGAL-*UPS1*(grey) or pGAL-*FUR4* (black) were grown to
18
19 570 exponential phase in galactose containing medium and used for measurement of
20
21 571 [¹⁴C] uracil uptake as described in Materials and Methods. Results are the average of
22
23 572 four measures (two measures in two independent experiments).
24
25
26
27 573

28
29 574 **Figure 2: Intracellular trafficking of AtUPS1 in yeast.**

30
31
32 575 A: *fur4*Δ strains transformed with pGAL-*UPS1* (triangle) or pGAL-*FUR4* (circle) were
33
34 576 grown with raffinose as a carbon source. Galactose was then added to induce
35
36 577 expression of *AtUPS1* and *FUR4*. The kinetics of plasma membrane delivery of
37
38 578 AtUPS1 and Fur4p was determined by quantification of [¹⁴C] uracil uptake every 30
39
40 579 minutes after galactose induction. Results at each time point are the average of two
41
42 580 independent measurements.
43
44
45

46 581 B: *fur4*Δ strains transformed with pGAL-*UPS1* (triangle) or pGAL-*FUR4* (circle) were
47
48 582 grown in galactose containing medium. Protein synthesis was inhibited by addition of
49
50 583 cycloheximide (CHX) (100μg/ml). Uracil uptake activity was measured at various time
51
52 584 points (two measurements) after CHX addition. Results are shown as the percentage
53
54 585 of initial activities.
55
56
57
58 586
59
60

1
2
3 587 **Figure 3: Expression of C-terminally GFP tagged AtUPS1 promotes ER**
4
5 588 **proliferation in yeast**
6

7
8 589 A: *fur4*Δ cells transformed with pGAL, pGAL-*UPS1-HA*, pGAL-*UPS1-GFP* and
9
10 590 *pCYC1-UPS1-GFP* were tested for growth on plates containing or not 5-fluorouracil
11
12 591 (0,75 μM).
13
14

15 592 B and C: *fur4*Δ cells transformed with pCYC-*UPS1-GFP*, pGAL-*UPS1-GFP* or pGAL-
16
17 593 *Fur4-GFP* were grown to mid exponential phase either in glucose, or in raffinose
18
19 594 containing medium in the case of strains bearing a plasmid with a GAL promoter.
20
21 595 Galactose was then added to induce *AtUPS1-GFP* or *Fur4-GFP* expression. At the
22
23 596 indicated times, after galactose addition or after growth in glucose containing media
24
25 597 (in the case of pCYC-*UPS1-GFP*), cells were observed by fluorescence microscopy
26
27 598 (B) and protein extracts were prepared, resolved by SDS PAGE and analysed by
28
29 599 Western immunoblotting using an anti-GFP antibody (C)
30
31
32
33

34 600 D: *fur4*Δ cells expressing pGAL and pGAL-*UPS1-GFP* grown overnight in galactose
35
36 601 containing media were processed for electron microscopy. White arrows indicate the
37
38 602 endoplasmic reticulum and N the nucleus.
39
40
41
42

43
44 604 **Figure 4: Intracellular fate of myc tagged version of AtUPS1**
45

46 605 A: *fur4*Δ cells transformed with pGAL, pGAL-*UPS1*, and pGAL-*UPS1^{myc}* were tested
47
48 606 for 5-fluorouracil (1 μM) sensitivity on plates.
49

50
51 607 B: [¹⁴C] uracil uptake activity of *fur4*Δ cells transformed with pGAL-*FUR4*, pGAL-
52
53 608 *UPS1* and pGAL-*UPS1^{myc}* grown to mid exponential phase on galactose containing
54
55 609 medium. Results are the average of two independent measures.
56

57
58 610 C: *fur4*Δ strains transformed with pGAL-*UPS1* (triangle) or pGAL-*UPS1^{myc}* (square)
59
60 611 were grown to mid log phase in raffinose containing medium and galactose was then

1
2
3 612 added to induce expression of the transporter. The kinetics of plasma membrane
4
5 613 delivery of AtUPS1 or Fur4p were determined by quantification of [¹⁴C] uracil uptake
6
7
8 614 at various times after galactose induction.
9

10 615 D: *fur4Δ* strains transformed with pGAL-UPS1 (triangle) or pGAL-UPS1^{myc} (square)
11
12 616 were grown in galactose containing medium. Uracil uptake activity was measured at
13
14
15 617 different time points after inhibition of protein synthesis by addition of CHX
16
17 618 (100μg/ml). Results are shown as the percentage of initial activity.
18

19
20 619 E: WT cells transformed with pGAL-UPS1^{myc} were grown to mid log phase in
21
22 620 raffinose containing medium. Galactose was then added to induce transporter
23
24 621 expression. Protein extracts were prepared at indicated times and proteins were
25
26 622 resolved by SDS PAGE and analysed by Western immunoblotting using an anti-myc
27
28 623 antibody to detect the transporter and an anti-Gas1p as a loading control.
29
30
31

32 624

33
34 625 **Figure 5: Intracellular localization of UPS1^{myc} after galactose induction.**

35
36 626 A: *fur4Δ* cells transformed with pGAL-UPS1^{myc} were grown overnight in raffinose
37
38 627 containing media. Galactose was added during exponential growth phase. Aliquots
39
40 628 were withdrawn at various time points, cells were fixed and processed for
41
42 629 immunofluorescence. AtUPS1^{myc} was detected using an anti-myc antibody as
43
44 630 described in Materials and Methods. The nuclei were stained using DAPI.
45
46 631 Fluorescence was observed under an Olympus microscope.
47
48
49

50
51 632 (Note that, as it is often the case for multicopy plasmid and galactose induction, only
52
53 633 a subset of the cells within the population was stained with the anti-myc antibody)

54
55 634 B: The same preparations as in (A) were also visualized using confocal microscopy.
56
57 635 One section is presented for each time point.
58
59

60 636

1
2
3 637 Figure 6: **Mutations in *RSP5* improve functional expression in yeast of tagged**
4
5 638 **and untagged UPS1**

6
7
8 639 A: *fur4* Δ , *rsp5* Δ *C2 fur4* Δ and *npi1 fur4* Δ cells transformed with pPGK-*UPS1*, pGAL-
9
10 640 *UPS1*, pGAL-*UPS1-GFP* or pGAL-*UPS1^{myc}* were grown in glucose containing
11
12 641 medium and spotted either on glucose (pPGK-*UPS1*) or on galactose containing
13
14 642 plates (pGAL plasmids) with or without 5-fluorouracil as indicated. Different 5FU
15
16 643 concentrations were used in order to differentiate optimally the growth of each of the
17
18 644 tested strains with regard to the various plasmids: concentration was lower in the
19
20 645 case of galactose-induced cells expressing untagged and myc-tagged AtUPS1 that
21
22 646 display greater uracil uptake activities than cells expressing GFP-tagged AtUPS1, or
23
24 647 untagged AtUPS1 under the control of the PGK promoter. In all cases, growth was
25
26 648 tested using a whole range of 5FU concentrations, and a selection of representative
27
28 649 plates is shown.

29
30
31
32
33
34 650 B: *fur4* Δ (triangle), *rsp5* Δ *C2 fur4* Δ (square) and *npi1 fur4* Δ (diamond) transformed
35
36 651 with pGAL-*UPS1-GFP* or pGAL-*UPS1^{myc}* were grown to mid log phase in raffinose
37
38 652 containing media and the expression of the various transporters was induced by
39
40 653 addition of galactose. Plasma membrane delivery of the transporters was assessed
41
42 654 by measuring uracil uptake activity at different time points after galactose addition.

43
44
45 655 C: Induction of AtUPS1^{myc} was monitored in *WT* and *npi1* cells by Western blot
46
47 656 analysis of aliquots withdrawn at several time points after addition of galactose.
48
49 657 Proteins were resolved by SDS polyacrylamide gel electrophoresis and analyzed by
50
51 658 immunoblotting with anti-myc antibodies for quantification of transporter expression
52
53 659 and anti-Gas1p as loading control.

54
55
56
57
58 660
59
60

661 **Acknowledgements**

662 We thank H. Riezman for the kind gift of antibodies, Antonia Kropfingher for editorial
663 assistance, and the members of RHT's laboratory for helpful discussions and
664 comments on the manuscript and. We are grateful to Sophie Le Panse for electron
665 microscopy. We also thank Jennifer Molinari, Youri Lokossa, Ludovic Warroux and
666 Yvonne Sauermann for technical help. This work was supported by a grant to M.D.
667 from the Deutsche Forschungsgemeinschaft (DE 817/1-1).The work done in RHT's
668 lab was supported by the Centre National de la Recherche Scientifique, the
669 Universities Paris 6 and Paris 7, by a grant from the Association pour la Recherche
670 contre le Cancer (ARC) (grant no. 3298), and by an European Union program
671 (EFFEXPORT, contract QLRT-2001-00533). Marine Froissard, Naïma Belgareh-
672 Touzé and Jennifer Molinari received fellowships from this program. We are
673 especially indebted to Bruno Andre, coordinator of the EFFEXPORT program, for his
674 constant support.

675

676 **References**

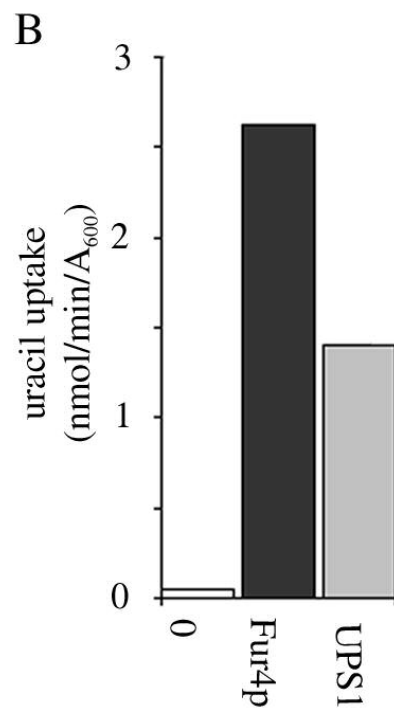
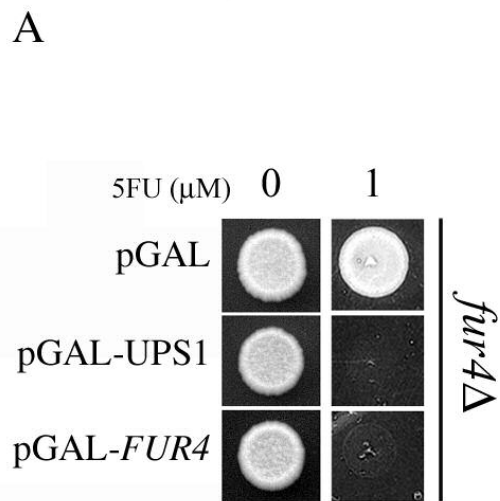
677

- 678 (1) Schwacke, R.; Schneider, A.; van der Graaff, E.; Fischer, K.; Catoni, E; M., D.;
679 Frommer, W.; Flugge, U.; Kunze, R. *Plant Physiol.* 2003, *131*, 16-26.
- 680 (2) Andre, B. *Yeast* 1995, *11*, 1575-611.
- 681 (3) Nelissen, B.; De Wachter, R.; Goffeau, A. *FEMS Microbiol Rev* 1997, *21*, 113-34.
- 682 (4) Van Belle, D.; Andre, B. *Curr Opin Cell Biol* 2001, *13*, 389-98.
- 683 (5) Winzeler, E. A.; Shoemaker, D. D.; Astromoff, A.; Liang, H.; Anderson, K.; Andre,
684 B.; Bangham, R.; Benito, R.;et al. *Science* 1999, *285*, 901-6.

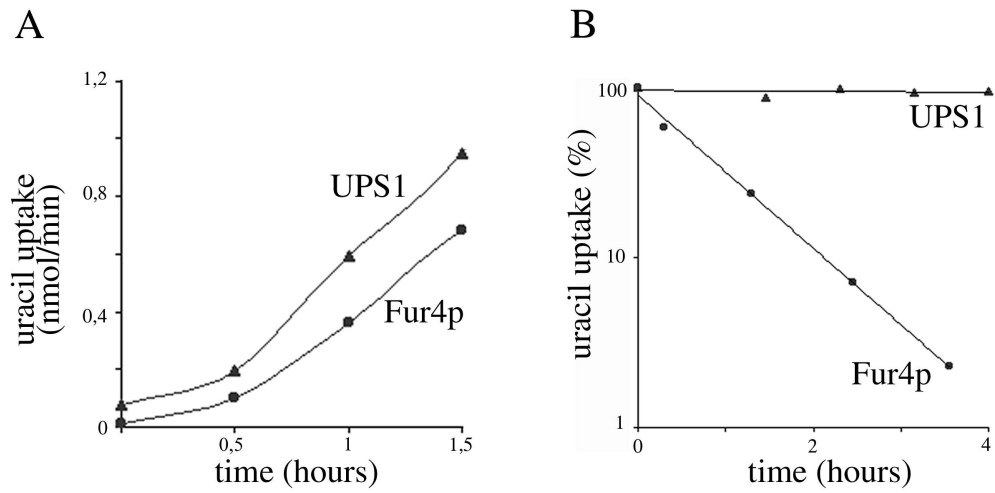
- 1
2
3 685 (6) Frommer, W. B.; Ninnemann, O. *Annu. Rev. Plant Physiol. Plant Mol. Biol.* 1995, 46,
4
5 686 419-444.
6
7
8 687 (7) Barbier-Brygoo, H.; Gaymard, F.; Rolland, N.; Joyard, J. *Trends Plant Sci* 2001, 6,
9
10 688 577-85.
11
12 689 (8) Dreyer, I.; Horeau, C.; Lemaillet, G.; Zimmermann, S.; Bush, D. R.; Rodriguez-
13
14 690 Navarro, A.; Schachtman, D. P.; Spalding, E. P.; Sentenac, H.; Gaber, R. F. *J. Exp.*
15
16 691 *Bot.* 1999, 50, 1073-1087.
17
18
19 692 (9) Bush, D. R. *Curr Opin Plant Biol* 1999, 2, 187-91.
20
21 693 (10) Palmgren, M. G.; Christensen, G. *J Biol Chem* 1994, 269, 3027-33.
22
23 694 (11) de Kerchove d'Exaerde, A.; Supply, P.; Dufour, J. P.; Bogaerts, P.; Thines, D.;
24
25 695 Goffeau, A.; Boutry, M. *J Biol Chem* 1995, 270, 23828-37.
26
27 696 (12) Niebauer, R. T.; Wedekind, A.; Robinson, A. S. *Protein Expr Purif* 2004, 37, 134-43.
28
29 697 (13) Makuc, J.; Cappellaro, C.; Boles, E. *FEMS Yeast Res* 2004, 4, 795-801.
30
31 698 (14) Wiczorke, R.; Dlugai, S.; Krampe, S.; Boles, E. *Cell Physiol Biochem* 2003, 13, 123-
32
33 699 34.
34
35 700 (15) Desimone, M.; Catoni, E.; Ludewig, U.; Hilpert, M.; Schneider, A.; Kunze, R.;
36
37 701 Tegeder, M.; Frommer, W. B.; Schumacher, K. *Plant Cell* 2002, 14, 847-56.
38
39 702 (16) Schmidt, A.; Su, Y. H.; Kunze, R.; Warner, S.; Hewitt, M.; Slocum, R. D.; Ludewig,
40
41 703 U.; Frommer, W. B.; Desimone, M. *J Biol Chem* 2004, 279, 44817-24.
42
43 704 (17) Haguenaer-Tsapis, R.; André, B. In *Control of transmembrane transport*; Boles E
44
45 705 and Krämer, R., Ed.; Springer Verlag, 2004.
46
47 706 (18) Garnier, C.; Blondel, M. O.; Haguenaer-Tsapis, R. *Mol Microbiol* 1996, 21, 1061-73.
48
49 707 (19) Galan, J. M.; Moreau, V.; Andre, B.; Volland, C.; Haguenaer-Tsapis, R. *J Biol Chem*
50
51 708 1996, 271, 10946-52.
52
53 709 (20) Rotin, D.; Staub, O.; Haguenaer-Tsapis, R. *J Membr Biol* 2000, 176, 1-17.
54
55
56
57
58
59
60

- 1
2
3 710 (21) Blondel, M. O.; Morvan, J.; Dupre, S.; Urban-Grimal, D.; Haguenaue-Tsapis, R.;
4
5 711 Volland, C. *Mol Biol Cell* 2004, 15, 883-95.
6
7
8 712 (22) Pizzirusso, M.; Chang, A. *Mol Biol Cell* 2004, 15, 2401-9.
9
10 713 (23) Hoppe, T.; Matuschewski, K.; Rape, M.; Schlenker, S.; Ulrich, H. D.; Jentsch, S. *Cell*
11
12 714 2000, 102, 577-86.
13
14
15 715 (24) Rodriguez, M. S.; Gwizdek, C.; Haguenaue-Tsapis, R.; Dargemont, C. *Traffic* 2003,
16
17 716 4, 566-75.
18
19
20 717 (25) Hein, C.; Springael, J. Y.; Volland, C.; Haguenaue-Tsapis, R.; Andre, B. *Mol*
21
22 718 *Microbiol* 1995, 18, 77-87.
23
24
25 719 (26) Wang, G.; McCaffery, J. M.; Wendland, B.; Dupre, S.; Haguenaue-Tsapis, R.;
26
27 720 Huibregtse, J. M. *Mol Cell Biol* 2001, 21, 3564-75.
28
29
30 721 (27) Moreau, V.; Galan, J. M.; Devilliers, G.; Haguenaue-Tsapis, R.; Winsor, B. *Mol Biol*
31
32 722 *Cell* 1997, 8, 1361-75.
33
34
35 723 (28) Volland, C.; Urban-Grimal, D.; Geraud, G.; Haguenaue-Tsapis, R. *J Biol Chem* 1994,
36
37 724 269, 9833-41.
38
39
40 725 (29) Dupre, S.; Haguenaue-Tsapis, R. *Mol Cell Biol* 2001, 21, 4482-94.
41
42
43 726 (30) Marchal, C.; Dupre, S.; Urban-Grimal, D. *J Cell Sci* 2002, 115, 217-26.
44
45
46 727 (31) Bugnicourt, A.; Froissard, M.; Sereti, K.; Ulrich, H. D.; Haguenaue-Tsapis, R.;
47
48 728 Galan, J. M. *Mol Biol Cell* 2004, 15, 4203-14.
49
50
51 729 (32) Dupre, S.; Urban-Grimal, D.; Haguenaue-Tsapis, R. *Biochim Biophys Acta* 2004,
52
53 730 1695, 89-111.
54
55
56 731 (33) Bachmair, A.; Novatchkova, M.; Potuschak, T.; Eisenhaber, F. *Trends Plant Sci* 2001,
57
58 732 6, 463-70.
59
60 733 (34) Morvan, J.; Froissard, M.; Haguenaue-Tsapis, R.; Urban-Grimal, D. *Traffic* 2004, 5,
734 383-92.

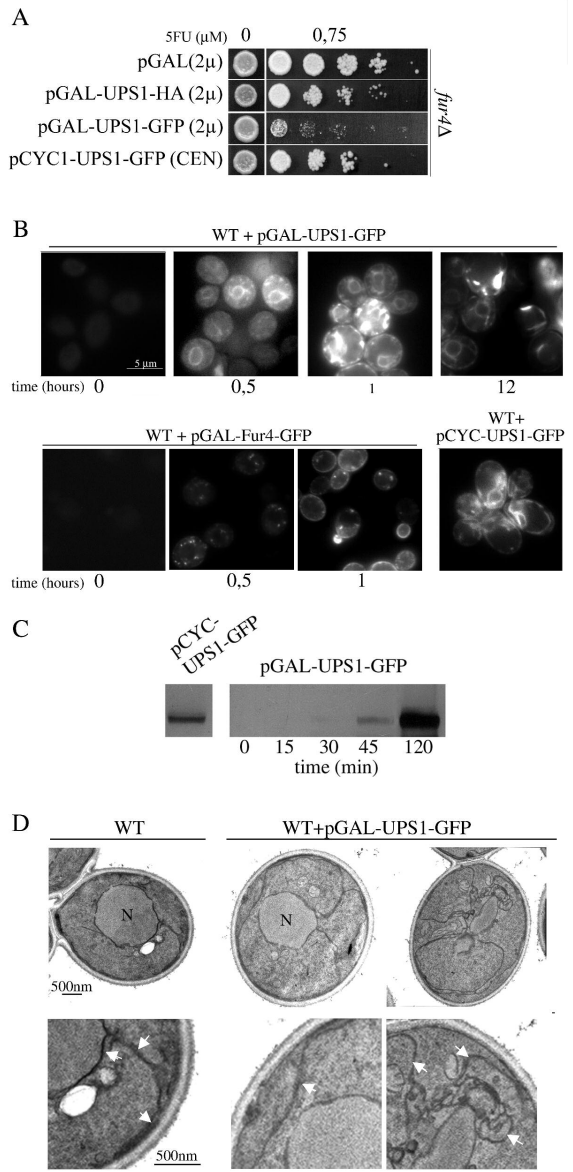
- 1
2
3 735 (35) Springael, J. Y.; De Craene, J. O.; Andre, B. *Biochem Biophys Res Commun* 1999,
4
5 736 257, 561-6.
6
7
8 737 (36) Dunn, R.; Hicke, L. *J Biol Chem* 2001, 276, 25974-81.
9
10 738 (37) Katzmann, D. J.; Sarkar, S.; Chu, T.; Audhya, A.; Emr, S. D. *Mol Biol Cell* 2004, 15,
11
12 739 468-80.
13
14
15 740 (38) Dunn, R.; Klos, D. A.; Adler, A. S.; Hicke, L. *J Cell Biol* 2004, 165, 135-44.
16
17 741 (39) Haynes, C. M.; Caldwell, S.; Cooper, A. A. *J Cell Biol* 2002, 158, 91-101.
18
19 742
20
21
22 743 (40) Soetens, O.; De Craene, J. O.; Andre, B. *J Biol Chem* 2001, 276, 43949-57.
23
24 744 (41) Gietz, D.; St Jean, A.; Woods, R. A.; Schiestl, R. H. *Nucleic Acids Res* 1992, 20,
25
26 745 1425.
27
28
29 746 (42) Wach, A. *Yeast* 1996, 12, 259-65.
30
31 747 (43) Maniatis, T.; Fritsch, E. F.; Sambrook, J. *Molecular Cloning: A Laboratory Manual*;
32
33 Cold Spring Harbor Laboratory: Cold Spring Harbor, N.Y., 1982.
34 748
35
36 749 (44) Cullin, C.; Minvielle-Sebastia, L. *Yeast* 1994, 10, 105-12.
37
38 750 (45) Niedenthal, R. K.; Riles, L.; Johnston, M.; Hegemann, J. H. *Yeast* 1996, 12, 773-86.
39
40 751 (46) Mumberg, D.; Muller, R.; Funk, M. *Gene* 1995, 156, 119-22.
41
42 752 (47) Rentsch, D.; Laloi, M.; Rouhara, I.; Schmelzer, E.; Delrot, S.; Frommer, W. B. *FEBS*
43
44 753 *Lett* 1995, 370, 264-8.
45
46
47
48 754 (48) Belgareh-Touze, N.; Avaro, S.; Rouille, Y.; Hoflack, B.; Haguenaer-Tsapis, R. *Mol*
49
50 755 *Biol Cell* 2002, 13, 1694-708.
51
52
53 756
54
55 757
56
57
58
59
60



Review

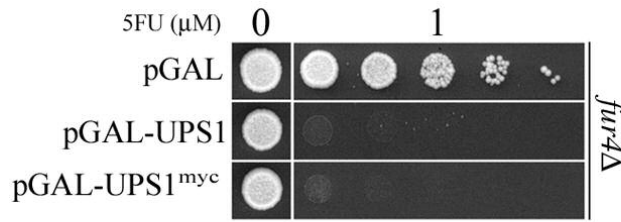


1
2
3
4
5
6
7
8
9
10
11
12
13
14
15
16
17
18
19
20
21
22
23
24
25
26
27
28
29
30
31
32
33
34
35
36
37
38
39
40
41
42
43
44
45
46
47
48
49
50
51
52
53
54
55
56
57
58
59
60

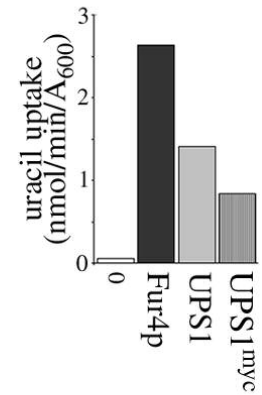


1
2
3
4
5
6
7
8
9
10
11
12
13
14
15
16
17
18
19
20
21
22
23
24
25
26
27
28
29
30
31
32
33
34
35
36
37
38
39
40
41
42
43
44
45
46
47
48
49
50
51
52
53
54
55
56
57
58
59
60

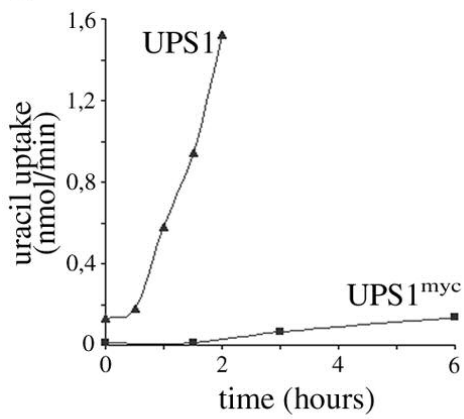
A



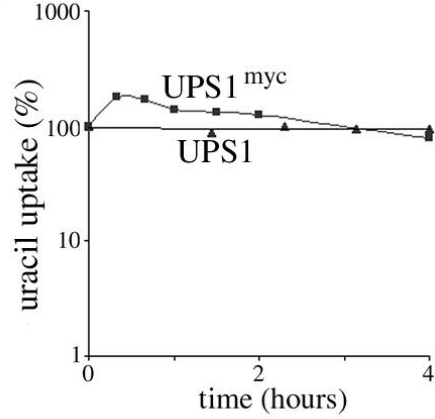
B



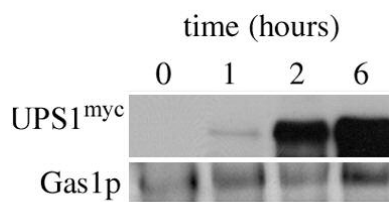
C

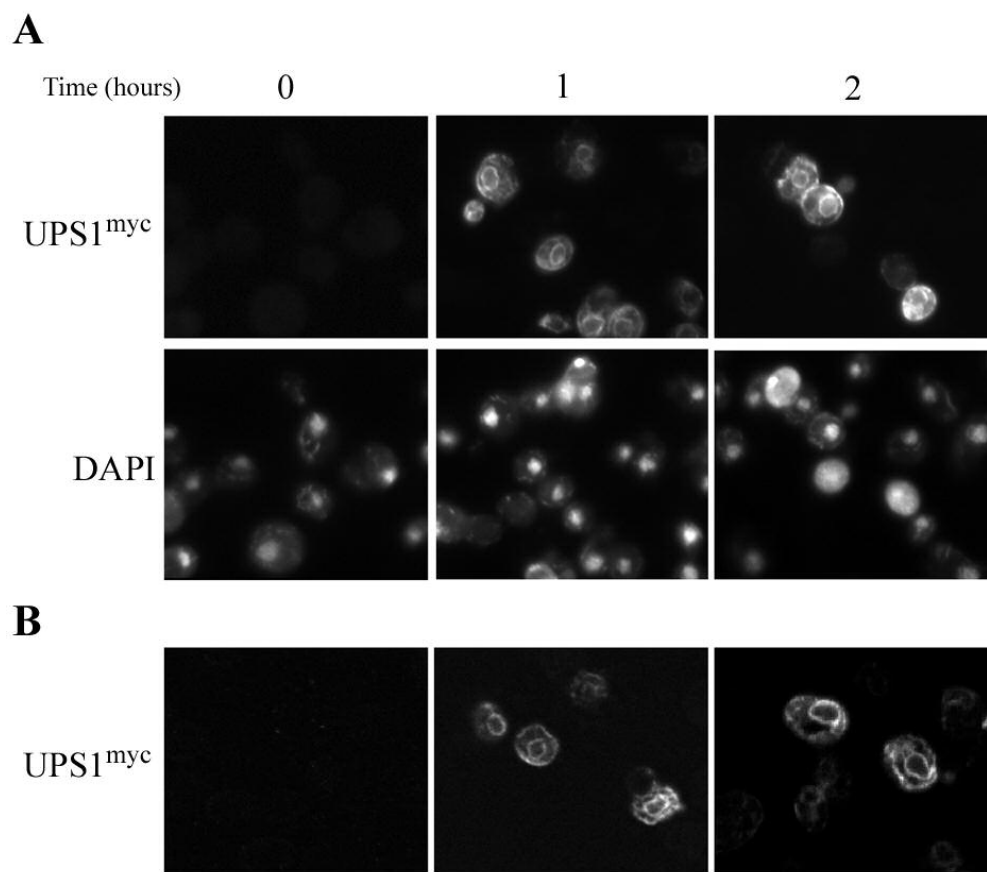


D

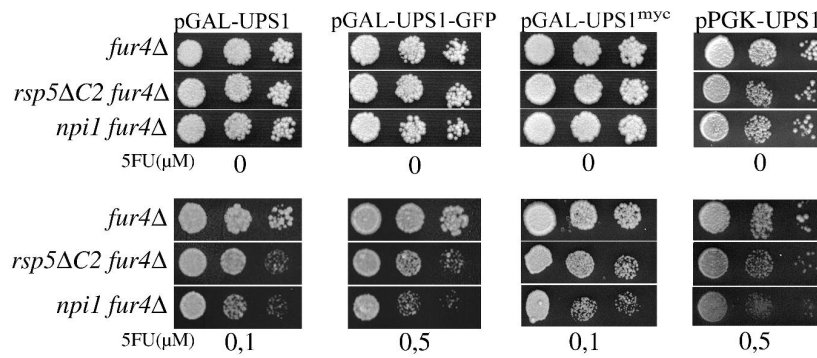


E

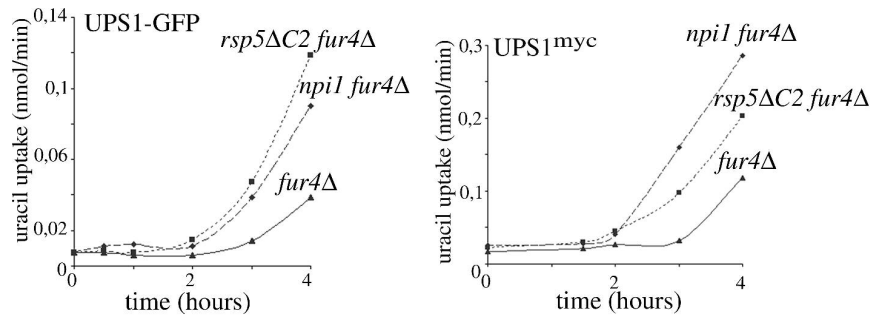




A



B



C

